Frontiers of Information Technology & Electronic Engineering
www.jzus.zju.edu.cn; engineering.cae.cn; www.springerlink.com
ISSN 2095-9184 (print); ISSN 2095-9230 (online)
E-mail: jzus@zju.edu.cn

Correspondence:

A compact ultra-wideband crossed-dipole antenna for 2G/3G/4G/IMT/5G customer premise equipment applications*

Jingli GUO[†1], Lun CUI[†‡1], Ying LIU[1], Baohua SUN[1], Xiaofeng LI[2]

[1]*Key Laboratory of Antennas and Microwave Technologies, Xidian University, Xi'an 710071, China*

[2]*Huawei Technologies Co., Ltd., Xi'an 710075, China*

[†]E-mail: guojl@xidian.edu.cn; ID_CLXX@163.com

Received Sept. 3, 2020; Revision accepted May 26, 2021; Crosschecked July 14, 2021; Published online Aug. 11, 2021

https://doi.org/10.1631/FITEE.2000456

1 Introduction

A compact ultra-wideband crossed-dipole antenna is proposed for 2G/3G/4G/IMT/5G customer premise equipment (CPE) applications. The arms of the crossed-dipole antenna are formed by step-shaped patches, and a wideband operation can be realized by properly selecting the order of the step-shaped patches; its bandwidth can be further enhanced by extending the end of crossed dipole downward. Each dipole is excited by a microstrip stub that is directly connected to a coaxial cable. Furthermore, a slotted rectangular parasitic patch is added beneath the crossed dipoles to further support a 5G sub-6-GHz band without additional space cost. The test results for the prototype of the proposed antenna show that the crossed-dipole antenna has a bandwidth of 147.3% (0.77–5.07 GHz) for return loss lower than 10 dB and an isolation higher than 20 dB between two ports.

The commercial use of 5G provides a huge opportunity for Internet of Things (IoT) applications (Duan, 2020). CPE can establish a wireless connection with a base station, and then turn the signals from the communication service providers into Wi-Fi signals; thus, consumers can access the Internet through Wi-Fi. This allows terminal devices to use Wi-Fi signals provided by 5G CPE to enjoy the convenience of a 5G system, even if they do not support the 5G standard. As the assignment of the 5G sub-6-GHz spectrum is different in different countries (e.g., China, 3.4–3.6 GHz and 4.8–5 GHz; Europe, 3.4–3.8 GHz) and the existing 2G/3G/4G/IMT system will still work in many regions for a long time, it is necessary to design wideband antennas that can cover both 2G/3G/4G/IMT and 5G spectra to support global large-scale 5G commercial use.

Crossed-dipole antennas are widely adopted according to their advanced transmission characteristics: they are superior in reducing multi-path fading (Wong, 2002) and channel capacity can be doubled compared with the case where only one polarization is considered (Zhang B et al., 2019).

Adding a parasitic element is widely done to enhance the crossed-dipole antenna bandwidth (Zhou and Li, 2011; Cui et al., 2017; Wu et al., 2018). By adding four pairs of parasitic elements on four corners of the crossed dipole, its 15-dB bandwidth is enhanced from 1.9–2.6 GHz to 1.7–2.75 GHz, which could meet the frequency requirement for a base station (Cui et al., 2017). However, to support International Mobile Telecommunication (IMT) services in a base station, Wu et al. (2018) added a parasitic loop, a parasitic disk, four parasitic strips, and four plumb strips to the crossed-dipole antenna to realize a

‡ Corresponding author

* Project supported by the National Natural Science Foundation of China (No. 61771395) and the Natural Science Basic Research Plan in Shaanxi Province, China (No. 2018JM6085)

ORCID: Jingli GUO, https://orcid.org/0000-0002-4515-8165; Lun CUI, https://orcid.org/0000-0002-4575-8064

bandwidth of 65.1% (1.4–2.75 GHz). These parasitic elements greatly increased the profile of the structure and made it hard to assemble. Some work has been done to widen the impedance bandwidth of a crossed dipole by modifying its arms (Cui et al., 2014; Li YZ et al., 2015; Li JY et al., 2016; Alieldin et al., 2018; Wen et al., 2018; Zhang YH et al., 2019). In Zhang YH et al. (2019), multiple modes in two designs were all excited using double-loop dipoles with stepped exponentially shaped arms, and the impedance bandwidth realized was 75.1% for 1.68–3.7 GHz and 91.8% for 2.38–6.42 GHz. The crossed dipoles designed in Alieldin et al. (2018) comprised an elliptical dipole, bowtie dipole, and cat-ear shaped arms, where each of them corresponded to the different resonances at a lower band (0.7–0.96 GHz, 31.3%), middle band (1.7–3 GHz, 55.3%), and 5G band (3.3–3.8 GHz, 14.1%). Although these two designs take 5G operation into consideration, neither of them can support the whole 2G/3G/4G band and 5G new radio (NR) band simultaneously.

We propose a compact ultra-wideband crossed-dipole antenna for 2G/3G/4G/IMT/5G CPE applications. The frequency band of B1 (0.82–0.96 GHz) and B2 (1.4–2.7 GHz) can be covered by selecting three-step-shaped patches as the arms of the crossed dipoles. A special parasitic patch is introduced below the center of the crossed dipoles to further broaden the frequency band of the antenna. The measurement results show that the proposed antenna can fully cover the bandwidth required by 2G/3G/4G/IMT and sub-6-GHz 5G systems, and that it is a promising candidate for future terminal devices.

2 Antenna structure

Fig. 1 shows the detailed geometry of the proposed wideband crossed-dipole antenna. The whole antenna is composed of a pair of end-extended crossed dipoles and a slotted rectangular parasitic patch. All elements of the crossed dipole are printed on a 100 mm×100 mm×0.8 mm substrate of FR4, with a relative dielectric permittivity of 4.4. The four three-step-shaped arms of the crossed dipole are diagonally arranged on the substrate to make full use of the limited space. Because these arms, which are printed on the lower surface of the substrate, need to be fed properly, four metallic vias are drilled on two microstrip stubs to excite the crossed-dipole antenna to realize ±45° polarization (P1 for +45° polarization, P2 for −45° polarization). In this way, a compact planar feeding structure can be realized, and the "bridge" feeding structure is no longer needed. According to the side view shown in Fig. 1b, each end of the dipole has a downward extension of 9.2 mm, which increases the electrical length of dipole to cover the lower band (B1); also, the slotted parasitic patch is added beneath the crossed dipoles to further cover B3.

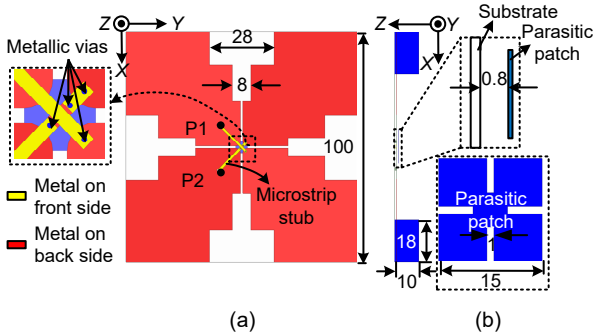

Fig. 1 Antenna structure: (a) top view; (b) side view (the unit is mm)

3 Design and analysis

3.1 2G/3G/4G/IMT antenna design

The design process of the proposed antenna and the corresponding S-parameters are shown in Fig. 2. First, the four arms of the crossed dipoles are started from a single-step-shaped patch (ant 1). The simulation results show that the impedance matching of the single-step-shaped cross dipole is not good, and that the isolation between P1 and P2 is worse than 20 dB in B2. By modifying the single-step-shaped dipole into a two-step-shaped dipole (ant 2), the impedance matching is improved in B1 and B2. Following the same method, the impedance matching can be further improved and B2 can be fully covered with reflection coefficients lower than −10 dB by a three-step-shaped dipole (ant 3). Meanwhile, the isolation for B2 is better than 22.5 dB and the isolation for B1 is even better than 40 dB. To fully cover B1, a downward extension at each end of the dipole is performed to increase the electrical length of the dipole.

The surface current distribution of ant 4 at 900 MHz is added to illustrate how higher isolation is

achieved in B1. As shown in Fig. 3, when P1 is fed, a strong current distribution can be found along the axial direction of dipole 1; also, the edges of dipole 2 comprise a strong induced current that is coupled from dipole 1. Taking the vector current distribution into consideration, the total equivalent current distribution on each arm of dipole 2 (black arrow) is exactly opposite to that of dipole 1 (white arrow), and this current is perpendicular to the microstrip feed line, which leads to weak current being induced to feed port 2 (Fig. 3b). Thus, higher isolation between dipoles 1 and 2 can be achieved. Fig. 4 shows the reflection coefficients of P1 in ant 4 with and without dipole 2. It is clear that the matching of ant 4 with dipole 2 is significantly better than that in the case of ant 4 without dipole 2, where the reflection coefficients are all worse than −10 dB over the band of interest. In fact, dipole 2 acts as two parasitic patches around dipole 1, which can be naturally used to broaden the bandwidth of dipole 1 to realize wideband operation.

3.2 5G antenna design

Fig. 5 shows how B3 can be fully covered by introducing a special parasitic patch. For crossed dipoles without loading any parasitic elements (ant 4), although two resonances can be found around 3.3 and 4.5 GHz, the impedance matching in B3 is rather poor. To improve the matching of B3, a square parasitic patch is first added beneath the feed point of the crossed dipoles where the parasitic patch can be easily activated by the strong current distributed around the feed point. The implementation of the parasitic patch greatly improves the matching in 3 and 4.3 GHz, and most of B3 can be covered. Further, by etching four slots on the parasitic patch along the gap between dipoles, another resonance is activated and B3 can be fully covered for reflection coefficients lower than

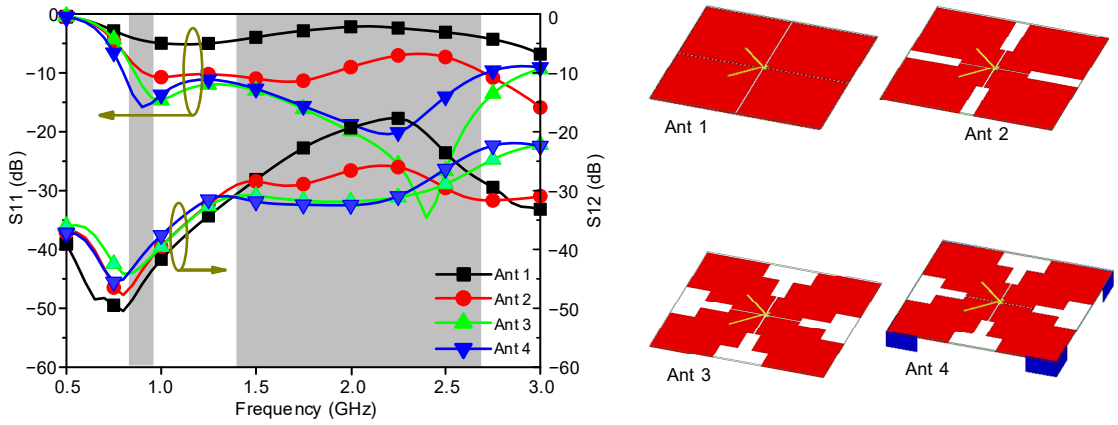

Fig. 2 Simulated S-parameters in the design process of the 2G/3G/4G/IMT antenna

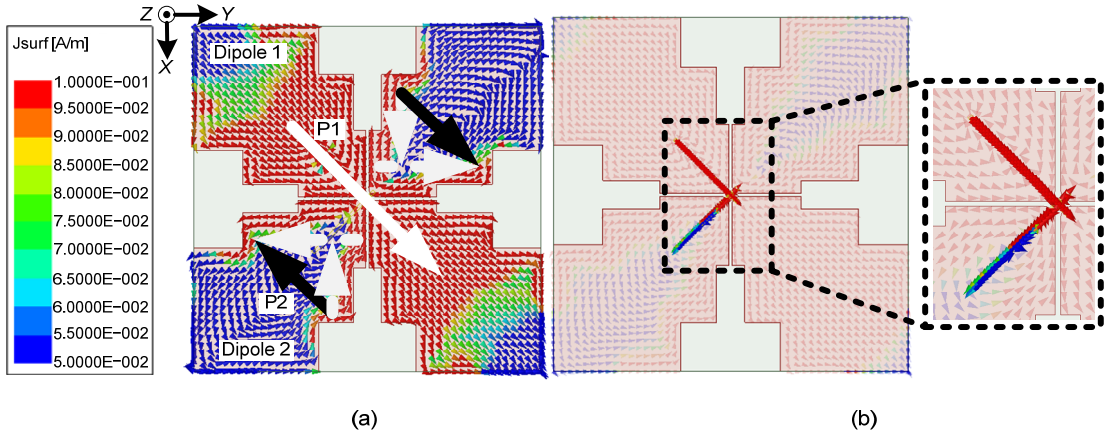

Fig. 3 Surface current vector distribution of ant 4 @900 MHz when P1 is activated: (a) dipole; (b) microstrip stub

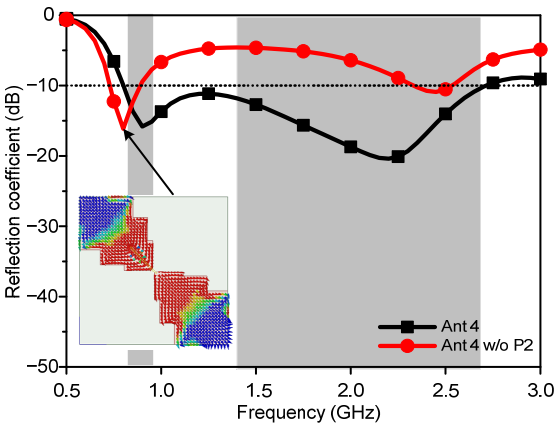

Fig. 4 Simulated reflection coefficients of P1 in ant 4 with and without (w/o) dipole 2

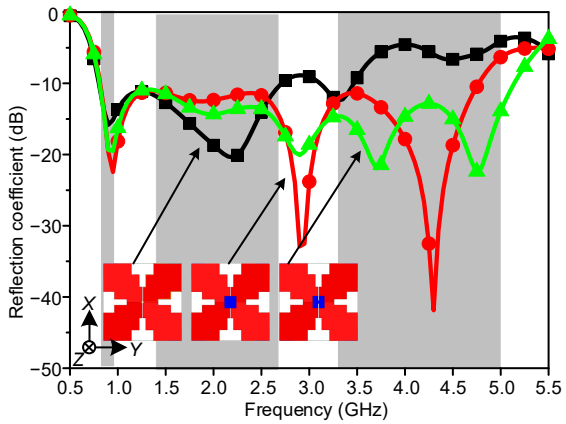

Fig. 5 Simulated reflection coefficients in the design process of the 5G band

−10 dB. Also, note that B3 can be tuned independently, because there is a negligible loading effect of the modified parasitic patch on the coverage of B1 and B2.

To clarify, the simulated surface current distributions at 3700 and 4800 MHz of the parasitic patch with and without the slot are presented in Fig. 6. According to Fig. 6a, before the slot is etched on the parasitic patch, the current concentrates mainly along the diagonal direction of the patch at two frequencies, and strong current distribution can be found at the four edges of the patch. After the parasitic patch is modified, the current distribution at 3700 MHz changes greatly as it is distributed mainly along the edges of the modified patch, so new resonance at 3700 MHz is excited. As for the resonance at 4800 MHz, a weak current distribution can be found along the edges of the patch, and the current is distributed mainly diagonally along the modified patch, which contributes to better matching at the higher band. In this way, B3 can be fully covered by the modified parasitic patch and L_{slot} is chosen to be 5 mm.

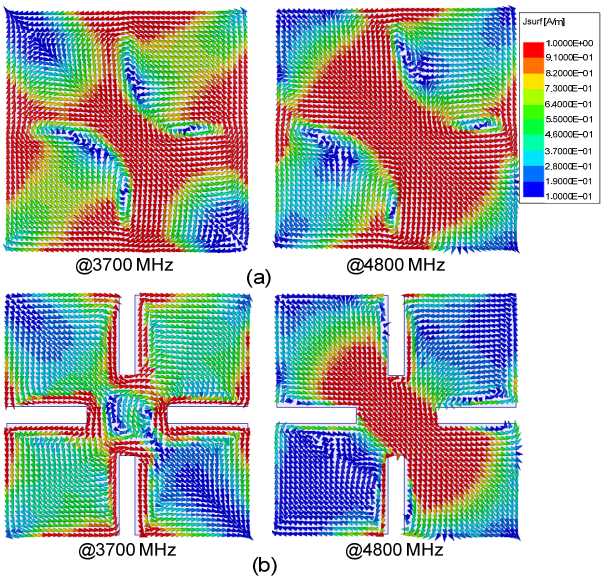

Fig. 6 Simulated surface current distribution at 3700 and 4800 MHz when P1 is excited: (a) parasitic patch without slot; (b) parasitic patch with slot

4 Experimental results

A prototype of the proposed antenna is fabricated and measured to validate the simulation results. As shown in Fig. 7, each port is fed by a flexible coaxial line, and four bent copper patches are soldered at each end of the dipole to further extend its length. The slotted parasitic patch is formed by cutting four slots on a copper patch, and it is fixed beneath the crossed dipole by sticking it on a small piece of foam.

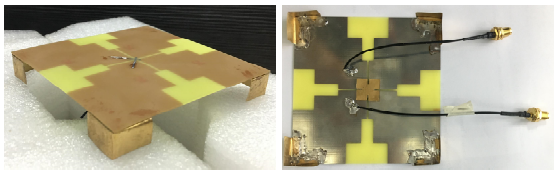

Fig. 7 Prototype of the proposed antenna: (a) perspective view; (b) backside view

The simulated and measured S-parameters are shown in Fig. 8. Although isolation differences and resonance shift are observed in B1 and B2 due to

fabrication tolerance (e.g., a gap is inevitable between the end of the dipole and the downward extension; the distance between the lower surface of the dipole and the slotted parasitic patch is not absolutely 0.8 mm because it is a handmade model), the discrepancy between the simulated and measured parameters is acceptable. It can be seen that both antennas can cover B1/B2/B3 and that the bandwidth of 147.3% (0.77–5.07 GHz) for reflection coefficients better than −10 dB can be realized; meanwhile, isolation higher than 20 dB is obtained within the band of interest.

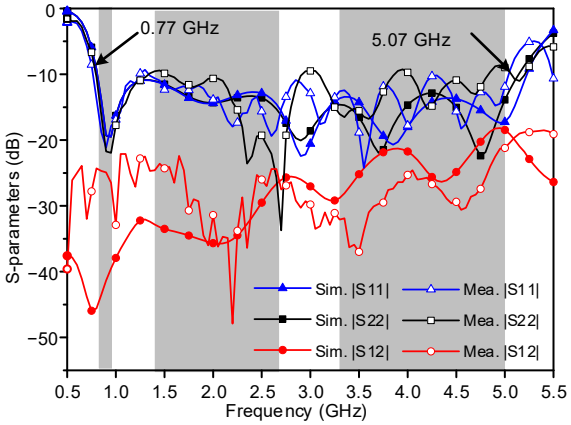

Fig. 8 Simulated and measured S-parameters

The simulated and measured radiation patterns at six different frequencies in the *ZOX* and *ZOY* planes are shown in Fig. 9. It can be seen that the radiation is bidirectional because there is no reflector added beneath the radiator that is normally used for backward radiation elimination. In addition, the co-polarization in the upper space will change to cross-polarization in the lower space due to the reversed propagation direction. Although there are some distortions caused by misalignment in antenna measurement, the measurement results agree well with the simulation results. For B1 and B2, the radiations are mainly toward the *Z* axis. Further, because the main radiator for B3 is not the crossed dipole but the parasitic patch beneath it and the higher frequency, the radiation for B3 is no longer along the *Z* axis but toward the *XOY* plane. In addition, the measurement results show that the gain ranges from 3 to 5 dBi in B1 and B2, and from 2 to 4 dBi in B3.

Comparisons between the proposed antenna and the designs in various references are shown in Table 1. We must clarify here that there is no reflector in our design because of the CPE applications, and the antennas in other references all have a reflector ground. This may be unfair, but it shows that our design is innovative. In a fair comparison, the normalization factor of antenna dimension λ_L represents the free-space wavelength at the lowest operating frequency in each design. It can be seen that the proposed antenna has the broadest bandwidth of 147.3% and has the most compact structure among the six designs, and an acceptable isolation (>20 dB) over the band of interest is also achieved with a simple structure.

5 Conclusions

A compact ultra-wideband crossed-dipole antenna for 2G/3G/4G/IMT/5G CPE applications is proposed. Better matching can be realized by adjusting the microstrip stub, and wideband operation is obtained with the help of three-step-shaped dipole arms and a slotted parasitic patch. The measurement results show that the proposed antenna could cover 2G/3G/4G/IMT/5G bands with a bandwidth of 147.3% (0.77–5.07 GHz) for return loss lower than

Table 1 Comparison between the proposed and referenced antennas

Reference	λ_L	Bandwidth	Isolation (dB)	Antenna structure
Wu et al., 2018	0.62×0.62×0.17	65.1% (1.40–2.75 GHz, 15 dB)	>30	Complex (10 parasitic patches)
	0.32×0.32 (planar)	63.0% (1.40–2.70 GHz, 15 dB)	>30	Simple (one parasitic patch)
Zhang YH et al., 2019	0.28×0.28 (planar)	91.8% (2.38–6.42 GHz, 10 dB)	>30	Simple
	0.28×0.28 (planar)	75.0% (1.68–3.7 GHz, 14 dB)	>30	
Alieldin et al., 2018	0.35×0.35 (planar)	31.3% (0.70–0.96 GHz, 10 dB); 55.3% (1.70–3.00 GHz, 10 dB); 14.0% (3.30–3.80 GHz, 10 dB)	>20	Simple
This paper	**0.24×0.24×0.03**	**147.3% (0.77–5.07 GHz, 10 dB)**	**>20**	**Simple (one parasitic patch)**

λ_L represents the free-space wavelength at the lowest operating frequency, and the unit is mm×mm or mm×mm×mm

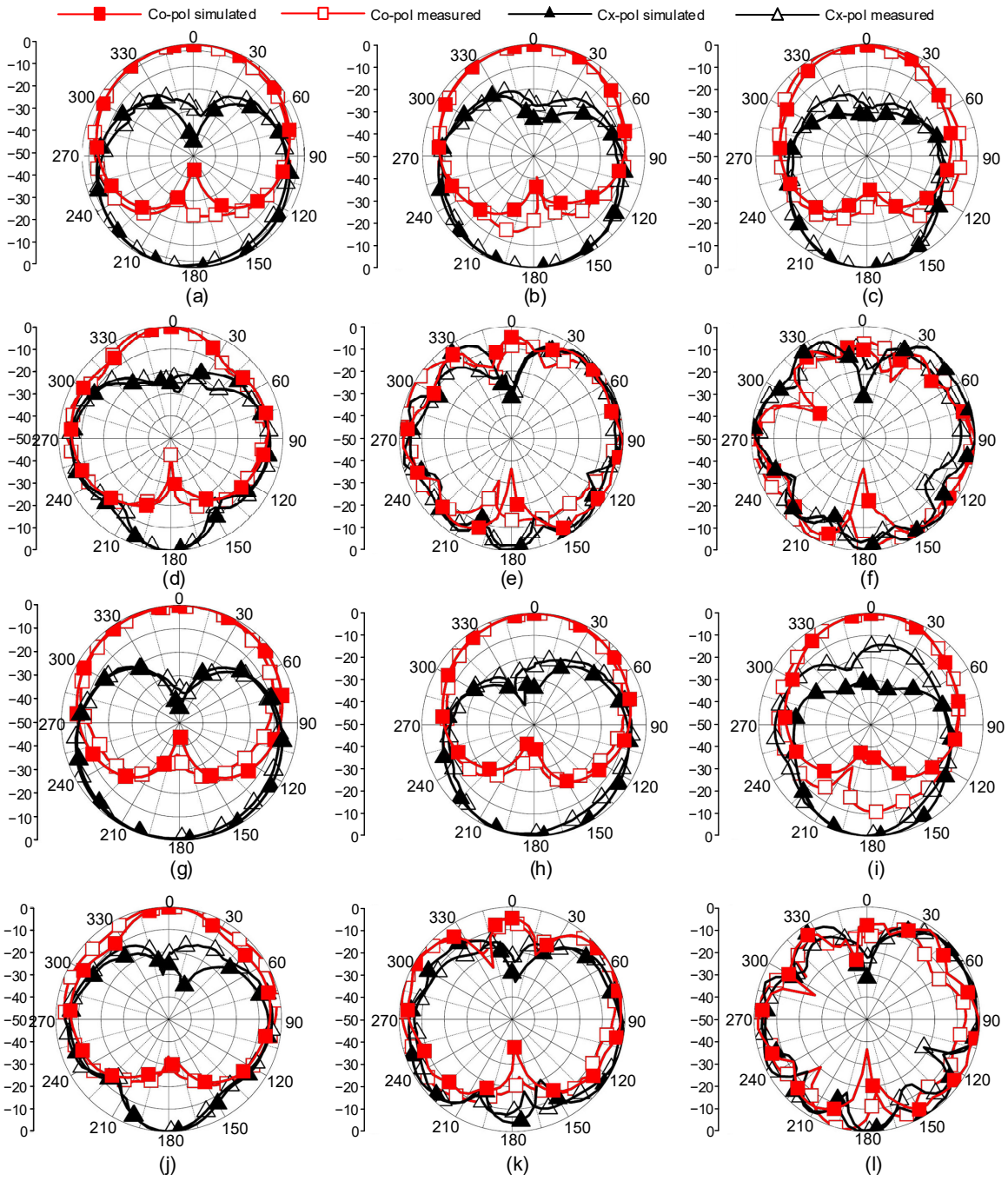

Fig. 9 Simulated and measured radiation patterns in the *ZOX* plane (a–f) and *ZOY* plane (g–l) when P1 is excited: (a) and (g) @900 MHz; (b) and (h) @1450 MHz; (c) and (i) @2200 MHz; (d) and (j) @2700 MHz; (e) and (k) @3500 MHz; (f) and (l) @4500 MHz

10 dB, and the isolation between two ports is higher than 20 dB; also, a stable radiation pattern is achieved. Due to its multiband operation and compact structure, the proposed crossed-dipole antenna is a promising candidate for future terminal devices.

Contributors

Jingli GUO and Lun CUI designed the research. Lun CUI drafted the manuscript. Jingli GUO, Ying LIU, Baohua SUN, and Xiaofeng LI helped organize the manuscript. Jingli GUO and Lun CUI revised and finalized the paper.

Acknowledgements

We would like to thank Kun LI from Huawei Technologies Co., Ltd. for his helpful suggestion and great support.

Compliance with ethics guidelines

Jingli GUO, Lun CUI, Ying LIU, Baohua SUN, and Xiaofeng LI declare that they have no conflict of interest.

References

Alieldin A, Huang Y, Boyes SJ, et al., 2018. A triple-band dual-polarized indoor base station antenna for 2G, 3G, 4G and sub-6 GHz 5G applications. *IEEE Access*, 6:49209-49216. https://doi.org/10.1109/ACCESS.2018.2868414

Cui YH, Li RL, Fu HZ, 2014. A broadband dual-polarized planar antenna for 2G/3G/LTE base stations. *IEEE Trans Antenn Propag*, 62(9):4836-4840. https://doi.org/10.1109/TAP.2014.2330596

Cui YH, Gao XN, Li RL, 2017. A broadband differentially fed dual-polarized planar antenna. *IEEE Trans Antenn Propag*, 65(6):3231-3234. https://doi.org/10.1109/TAP.2017.2694884

Duan BY, 2020. Evolution and innovation of antenna systems for beyond 5G and 6G. *Front Inform Technol Electron Eng*, 21(1):1-3. https://doi.org/10.1631/FITEE.2010000

Li JY, Xu R, Zhang X, et al., 2016. A wideband high-gain cavity-backed low-profile dipole antenna. *IEEE Trans Antenn Propag*, 64(12):5465-5469. https://doi.org/10.1109/TAP.2016.2620607

Li YZ, Liang XL, Bai XD, et al., 2015. An ultra-wideband cross-dipole antenna with wide beam for dual-polarization applications. Proc IEEE Int Symp on Antennas and Propagation & USNC/URSI National Radio Science Meeting, p.2027-2028. https://doi.org/10.1109/APS.2015.7305403

Wen LH, Gao S, Luo Q, et al., 2018. Compact dual-polarized shared-dipole antennas for base station applications. *IEEE Trans Antenn Propag*, 66(12):6826-6834. https://doi.org/10.1109/TAP.2018.2871717

Wong KL, 2002. Compact and Broadband Microstrip Antennas. John Wiley & Sons, Inc., New York, USA, p.10.

Wu LJ, Li RL, Qin Y, et al., 2018. Bandwidth-enhanced broadband dual-polarized antennas for 2G/3G/4G and IMT services. *IEEE Antenn Wirel Propag Lett*, 17(9):1702-1706. https://doi.org/10.1109/LAWP.2018.2864185

Zhang B, Liu W, Lan X, 2019. Orthogonally polarized dual-channel directional modulation based on crossed-dipole arrays. *IEEE Access*, 7:34198-34206. https://doi.org/10.1109/ACCESS.2019.2903909

Zhang YH, Zhang YH, Li DT, et al., 2019. Ultra-wideband dual-polarized antenna with three resonant modes for 2G/3G/4G/5G communication systems. *IEEE Access*, 7:43214-43221. https://doi.org/10.1109/ACCESS.2019.2906389

Zhou SG, Li JY, 2011. Low-profile and wideband antenna. *IEEE Antenn Wirel Propag Lett*, 10:373-376. https://doi.org/10.1109/LAWP.2011.2148688